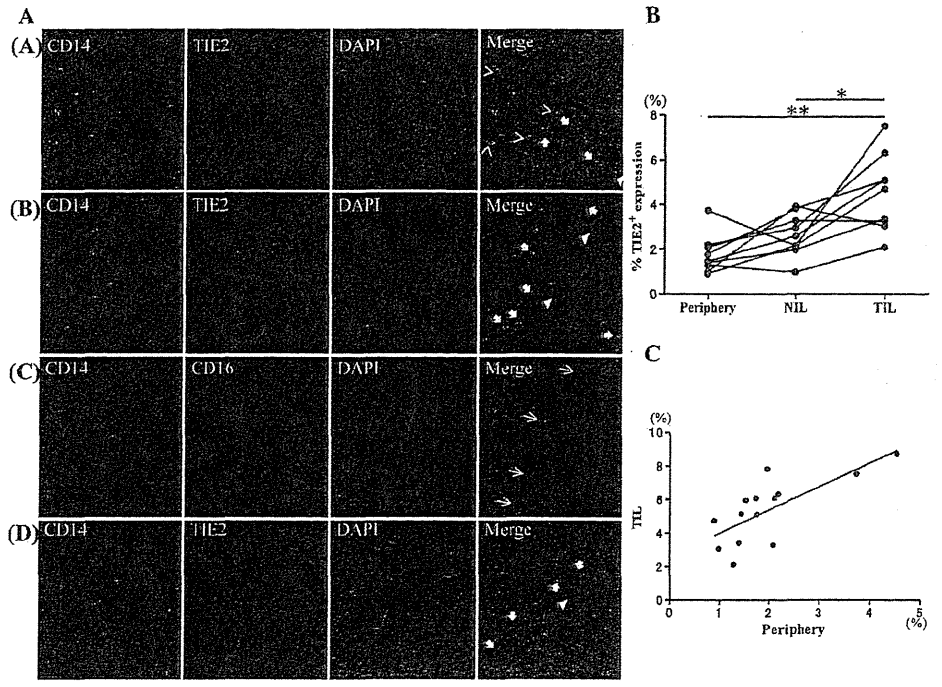

Fig. 3: TEMs are observed in perivascular areas of HCC tissue, and their frequency is higher in HCC tissue than in the periphery.

A. Immunofluorescence staining was performed as described in Materials and Methods. The staining for CD14 (green), CD16 (red) and TIE2 (red) identifies CD14+TIE2-, CD14+TIE2+, CD14+CD16- cells and CD14+CD16+ monocytes in human liver tissue (blue: nuclei counterstained with Dapi). Representative results of the resected samples obtained from 12 HCC patients are shown. The panels show CD14+TIE2+ cells (A, B, D) and CD14+CD16+ cells (C) in the perivascular area of HCC tissue (magnification, 400×), Bold arrows depict CD14+TIE2+ cells, thin arrows CD14+CD16+ cells, bold arrowheads vascular endothelial cells (TIE2+CD14-) and thin arrowheads CD14+TIE2- cells.

B. The frequencies of TEMs in 9 patients with HCC are compared for those in the peripheral blood or in the liver. Liver-infiltrating leukocytes are divided into two distinct groups: leukocytes infiltrating non-tumor tissue (NIL) and tumor-infiltrating leukocytes (TIL). These cells were stained using anti-human CD14, CD16 and TIE2 mAbs. The analyses were performed as described in Materials and Methods. The samples were obtained from nine patients who underwent tumor resection. *: $p<0.05$, **: $p<0.0005$, by Paired t-test.

C. The correlation is analyzed between the frequencies of TEMs in PBMC and those in tumor-infiltrated lymphocytes. Analysis (n=14) was based on Pearson's correlation coefficient. $P = 0.003$, $R2 = 0.53$.

254x190mm (300 x 300 DPI)

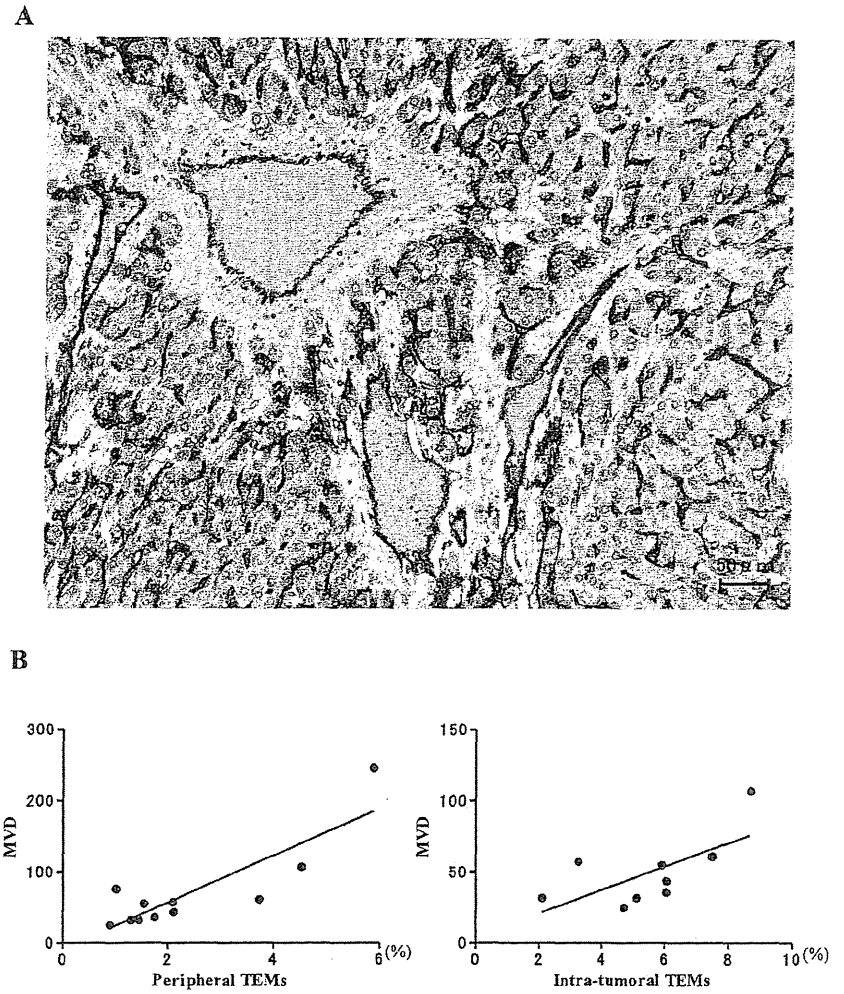

Fig. 4: The degree of microvessels in HCC is correlated with the frequency of TEMs
A. Assessment of neo-vascularization in HCC tissue was performed by staining CD34+ cells in the resected samples obtained from patients with HCC. Immunohistochemical staining for CD34 was done as described in Materials and Methods. The CD34+ cells were mainly confined to the cytoplasm of vascular endothelial cells as brownish yellow granules. Microvessels were represented by brownish yellow capillaries or small cell clusters. Representative results are shown. The panel shows a tumor cell area of a high grade.
B. The correlation is analyzed between TEM frequencies and the counts of CD34+ cells (MVD values) in relevant patients. The panels show the correlation of peripheral (left: n=11) or intra-tumoral TEM frequencies (right: n=9) and MVD ($p = 0.0009$, $R2 = 0.72$ and $p = 0.04$, $R2 = 0.44$, respectively). Analysis was based on Pearson's correlation coefficient.
190x254mm (300 x 300 DPI)

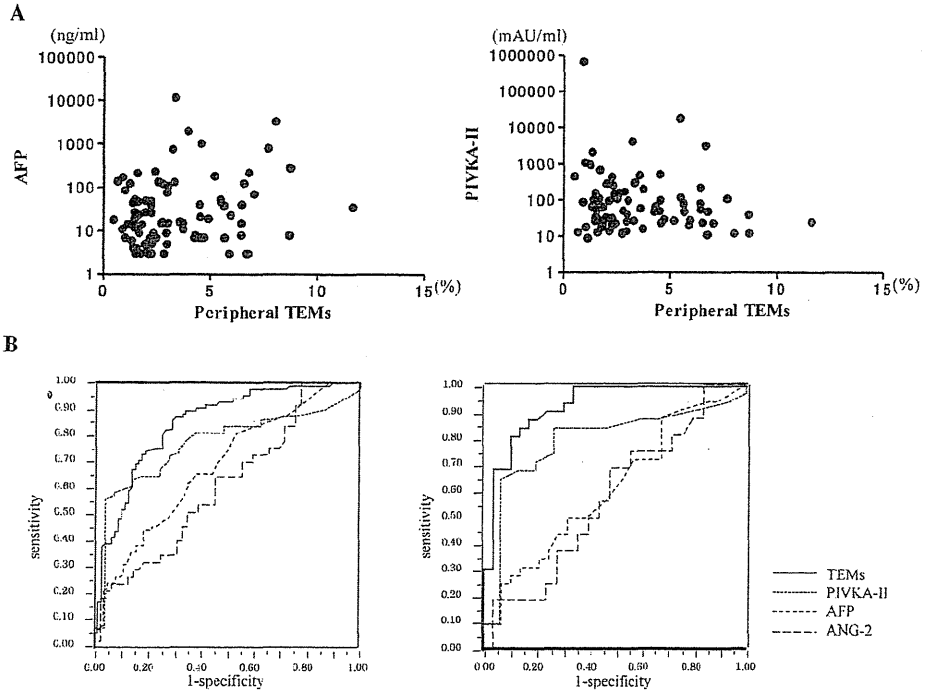

Fig. 5: Frequency of TEMs is superior as a diagnostic for HCC to common tumor markers or angiogenesis factor.

A. Correlation between TEM frequency and AFP (n=87) or PIVKA-II (n=81) was analyzed using Pearson's correlation coefficient. P = 0.45, R2 = 0.007 or P = 0.27, R2 = 0.02, respectively.

B. ROC analyses were performed in order to assess the diagnostic value of TEM frequency for differentiating HCC (n=89) from chronic liver disease (CLD, n=79) or liver cirrhosis (LC, n=30). The left panel shows the diagnostic value of TEMs, PIVKA-II, AFP and angiopoietin-2 (ANG-2) for HCC from CLD and the right panel shows those for HCC from LC, respectively.

254x190mm (300 x 300 DPI)

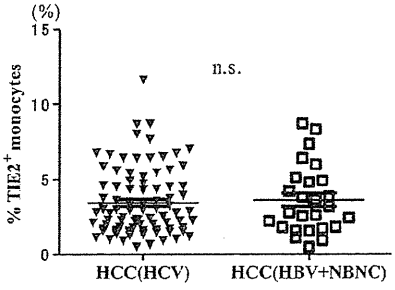

Supplementary figure 1: Frequency of TEMs is comparable in HCC patients regardless of etiology. The frequencies of peripheral TEMs are shown for HCC patients with or without HCV infection (n=89 and n=26, respectively). The group without HCV infection included patients with HBV infection or those without HBV nor HCV (HBV-HCC and Non-B, Non-C [NBNC] HCC patients). n.s., not significant by Mann-Whitney non-parametric U test.
254x190mm (300 x 300 DPI)

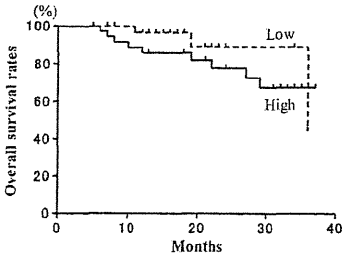

Supplementary figure 2: Peripheral frequency of TEMs is not related to the overall survival in patients with HCC.

In patients with HCC who underwent RFA or the operation, the overall survival rate after the treatment was compared between those with TEMhigh (frequency of TEMs≥2.75; n=45) and TEMlow (frequency of TEMs < 2.75; n=44) using the Kaplan-Meier method, with the log-rank test for comparison. TEMhigh and TEMlow , see Table 2. P=0.36

254x190mm (300 x 300 DPI)

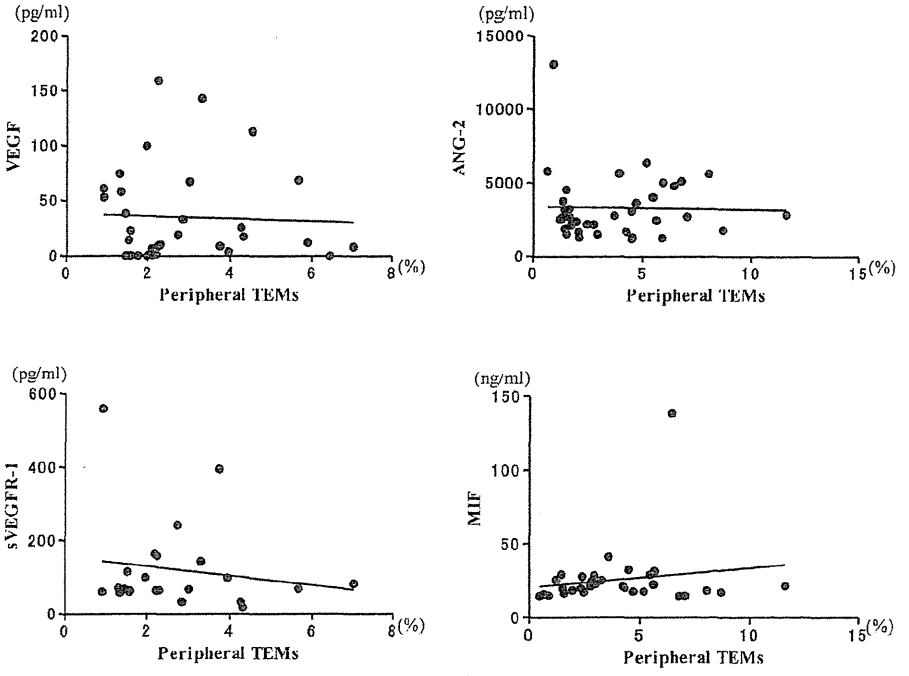

Supplementary figure 3: All plots indicate the correlation between TEM frequency and VEGF, ANG-2, sVEGFR-1 or MIF. The numbers of patients examined were 32, 37, 23 and 31, respectively. Analyses were based on Pearson's correlation coefficient.
254x190mm (300 x 300 DPI)

Virology 432 (2012) 452–459

Contents lists available at SciVerse ScienceDirect

Virology

journal homepage: www.elsevier.com/locate/yviro

Interferon-α suppresses hepatitis B virus enhancer II activity via the protein kinase C pathway

Takatoshi Nawa [a,1], Hisashi Ishida [a,1], Tomohide Tatsumi [a], Wei Li [a], Satoshi Shimizu [a], Takahiro Kodama [a], Hayato Hikita [a], Atsushi Hosui [a], Takuya Miyagi [a], Tatsuya Kanto [a], Naoki Hiramatsu [a], Norio Hayashi [b], Tetsuo Takehara [a,*]

[a] Department of Gastroenterology and Hepatology, Osaka University Graduate School of Medicine, 2-2 Yamadaoka, Suita, Osaka 565-0871, Japan
[b] Kansai-Rosai Hospital, Amagasaki, Hyogo 660-8511, Japan

ARTICLE INFO

Article history:
Received 12 April 2012
Returned to author for revisions
3 May 2012
Accepted 1 July 2012
Available online 24 July 2012

Keywords:
HBV
Enhancer II
Interferon-α
Protein kinase C

ABSTRACT

HBV has two enhancer (En) regions each of which promotes its own transcription. En II regulates production of pregenomic RNA, a key product of HBV replication, more strongly than En I. Although IFN-α has been found to suppress En I activity, its effect on En II activity has not been examined. Here we used luciferase assay to demonstrate that IFN-α suppresses En II activity. Analysis with several deletion/mutation constructs identified two major segments, nt 1703–1727 and nt 1746–1770, within the En II sequence as being responsible for the suppressive effects of IFN-α. Pre-treatment with protein kinase C (PKC) inhibitors blocked this effect regardless of the expression levels of phospho-STAT1 and Mx upon IFN-α stimulation. These results indicate that IFN-α suppresses En II activity via the PKC pathway, which may be an alternative suppressive pathway for HBV replication. (136 words).

Introduction

Hepatitis B virus (HBV) causes acute and chronic hepatitis in humans, and chronic infection is closely associated with the development of liver cirrhosis and hepatocellular carcinoma (Lok and McMahon, 2009). HBV has a partially double-stranded 3.2-kb DNA genome (relaxed circular (RC) DNA) in its nucleocapsid. When HBV invades host cells, RC-DNA is converted into a plasmid-like covalently closed circular DNA (cccDNA) inside the nucleus. From the cccDNA, the 3.5-, 2.4-, 2.1-, and 0.8-kb mRNAs are transcribed by cellular RNA polymerase II (Beck and Nassal, 2007). Among these RNAs, 3.5-kb pregenomic RNA (pgRNA) serves as the template of reverse transcription for synthesis of negative-strand DNA. Thus, transcription of pgRNA from cccDNA is one of the key steps in HBV replication.

In the HBV genome, there are four promoters (CP, SPI, SPII, and XP) and two transcriptional enhancer regions. Both enhancers stimulate transcription from the promoters (Antonucci and Rutter, 1989; Moolla et al., 2002; Su and Yee, 1992; Vannice and Levinson, 1988; Yee, 1989). Enhancer I (En I), which is located upstream of the X gene, activates transcription in a relatively cell-independent manner (Vannice and Levinson, 1988). In contrast, enhancer II (En II) (Fig. 1), located just upstream of CP, specifically activates transcription in hepatocytes (Wang et al., 1990; Yee, 1989; Yuh and Ting, 1990). Hepatocytes selectively express transcription factors which activate En II activity, such as HNF1 (Wang et al., 1998), HNF3 (Johnson et al., 1995; Li et al., 1995), HNF4 (Guo et al., 1993; Raney et al., 1997), CCAAT/enhancer binding protein (C/EBP) (López-Cabrera et al., 1990, 1991; Yuh and Ting, 1991) and FTF (Ishida et al., 2000; Li et al., 1998). This characterizes En II as a hepatocyte-specific *cis*-acting element. A previous report showed that, upon transfection with HBV genome, human hepatic cells, but not non-hepatic cells, were able to express pgRNA (Sureau et al., 1986). For this reason, En II is considered to regulate the production of pgRNA more strongly than En I (Yee, 1989).

Interferon-α (IFN-α) has been used as an anti-viral agent against HBV. It suppresses HBV viral load and ameliorates hepatic inflammation (Jonas et al., 2010; Liaw, 2009). Type I IFN activates the Janus kinase (JAK) bound to the cytoplasmic domain of its receptor. JAK phosphorylates transcription factors such as signal transducers and activators of transcription (STAT) 1 and STAT2. Phosphorylated STAT1 and STAT2 bind to IFN regulatory factor 9 (IRF9). These transcription factors form a complex, IFN-stimulated gene factor 3 (ISGF3). This complex binds to IFN stimulation response element (ISRE) in the promoter region of various genes, and activates interferon-stimulated genes (ISGs) (Der et al., 1998). Some of the ISGs including RNA-activated protein kinase (PKR), 2′,5′-oligoadenylate synthetases (OAS), and Mx have been shown to possess antiviral activity. ISG induction by type I IFN is considered to be the main pathway to suppressing viral replication.

* Corresponding author. Fax: +81 6 6879 3629.
E-mail address: takehara@gh.med.osaka-u.ac.jp (T. Takehara).
[1] T.N. and H.I. contributed equally to this work and share first authorship.

0042-6822/$ - see front matter © 2012 Elsevier Inc. All rights reserved.
http://dx.doi.org/10.1016/j.virol.2012.07.002

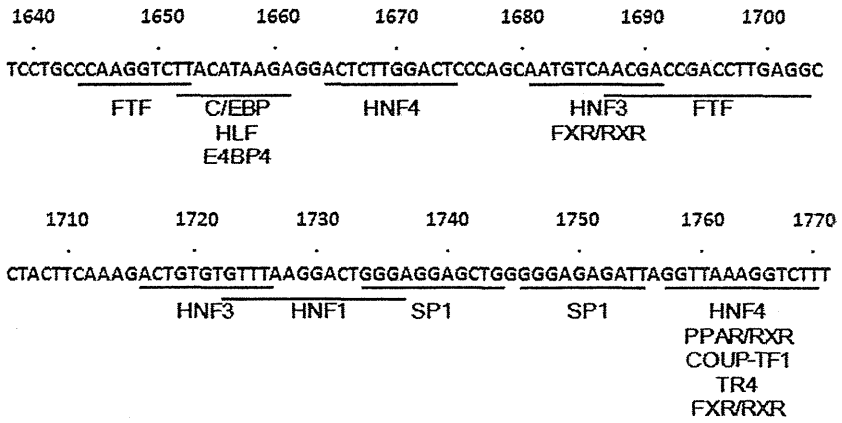

Fig. 1. Nucleotide sequences of the HBV En II region. The HBV sequence used in this study was of the *adw2* subtype (GenBank accession no. X02763). Numbering of the HBV sequence started at the unique *EcoRI* site. The underlined sequences represent the transcription factor binding sites mentioned in previous reports.

Type I IFN has been reported to inhibit HBV En I and core promoter activities (Nakao et al., 1999; Romero and Lavine, 1996; Schulte-Frohlinde et al., 2002; Tur-Kaspa et al., 1990). Nakao et al. demonstrated that IFN-α suppressed En I transcriptional activity by the binding of ISGF3 to the ISRE-like sequence in En I region (Nakao et al., 1999). However, there has been no study on the effect of IFN-α on HBV En II activity. In this study, we demonstrated that IFN-α suppressed En II activity via activation of PKC. Notably, STAT1 activation and ISG induction may be dispensable for IFN-α-mediated suppression of En II activity. This might shed light on understanding the inhibition of HBV replication by IFN-α.

Results

En II activity is down-regulated by IFN-α

We constructed a luciferase gene expression vector by inserting the En II sequence (nt 1640 to 1771) into pGL4LUC (pGL4LUC-En II). Huh-7 cells were transfected with pGL4LUC or pGL4LUC-En II, treated with or without IFN-α, and luciferase activities were evaluated. Insertion of En II increased the luciferase activity (about 228-fold) (Fig. 2A). IFN-α down-regulated the luciferase activity of pGL4LUC-En II, but did not affect that of pGL4LUC (Fig. 2B). This result suggested that IFN-α inhibited the activity of En II, and we examined the time course of IFN-α-induced suppression of En II activity. The suppressive effect of IFN-α on En II activity appeared at 3 h after administration of IFN-α, peaked at 6–12 h, and was gradually attenuated (Fig. 2C). Next, dose-response analysis showed that the En II activity was down-regulated by IFN-α in a dose-dependent manner, with the maximal suppressive effect at 300–1000 IU/m (Fig. 2D). We also examined the IFN-α-mediated suppression of En II activity in other hepatoma cell lines, PLC/PRF/5 and Hep3B. IFN-α significantly suppressed En II activities in both these cell lines (Fig. 2E). We next assessed whether or not IFN-α regulated HBV transcription in the HBV genome transfected cells by RT-PCR. HBV-RNA levels were significantly reduced by IFN-α (Fig. 2F). These results indicate that IFN-α suppresses HBV En II activity as well as its expression at a transcriptional level.

Both nt 1703–1727 and nt 1746–1770 within the En II region are required for suppression of En II activity by IFN-α

To determine the region responsible for the inhibitory effect of IFN-α on En II activity, we divided the En II sequence into six segments (Fig. 3A), and constructed plasmids containing En II sequences with deletion of each segment (pGL4LUC-En II-D1∼6). Huh-7 cells were transfected with these deleted constructs, treated with IFN-α, and then assayed for luciferase activity. None of the deletions could restore the suppressive activity by IFN-α (Fig. 3B), suggesting that there are several responsible regions for the IFN-α-induced suppression of En II activity. Next, we constructed plasmids containing four iterations of each segment within the En II sequence in tandem (pGL4LUC-En II-T1∼6) to examine the contribution of individual short fragments. IFN-α significantly suppressed the activities of pGL4LUC-En II-T2, T3, T4, T5 and -T6 in luciferase assay. Among them, the activities of pGL4LUC-En II-T4 and -T6 showed the largest suppression by IFN-α (Fig. 3C). On the basis of this result, we constructed a luciferase reporter vector with deletions of both segment 4 (nt 1703–1727) and segment 6 (nt 1746–1770) (pGL4LUC-En II-D4+6). The activity of this dual-deleted construct did not show a significant change due to IFN-α (Fig. 3D). These results suggest that both nt 1703–1727 and nt 1746–1770 within the En II region are required for the suppression of En II activity by IFN-α.

IFN-α-mediated suppression of En II activity is dependent on JAK activation

IFN-induced signal transduction occurs through the sequential activation of JAKs and STATs (Darnell et al., 1994). We examined the role of JAK in the inhibition of En II activity. JAK inhibitor alone did not affect En II activity. But the pre-treatment of the cells with JAK inhibitor completely blocked the suppressive effect of IFN-α on En II activity (Fig. 4A). The effect of JAK inhibitor was confirmed by the reducion of Mx induction in Western blot analysis (Fig. 4B). This result demonstrates that JAK activation is necessary for the IFN-α-induced suppression of En II activity.

The PKC pathway is involved in IFN-α-mediated suppression of En II activity

Previous reports demonstrated that type I IFN activated various kinases such as MAPK family members (MEK/ERK and p38 MAPK) (David et al., 1995; Goh et al., 1999), PI3K/Akt (Uddin et al., 1995), JNK (Caraglia et al., 1999) and protein kinase C (PKC) (Uddin et al., 2002). Here we examined the involvement of alternative pathways by pre-treatment with inhibitors for various kinases, including MEK, p38 MAPK, PI3K/Akt, JNK and PKC. The name of each inhibitors and its target kinase is commented in Table 1. As shown in Fig. 5A, only staurosporine, a PKC inhibitor, blocked the inhibitory effect of IFN-α, and other inhibitors did

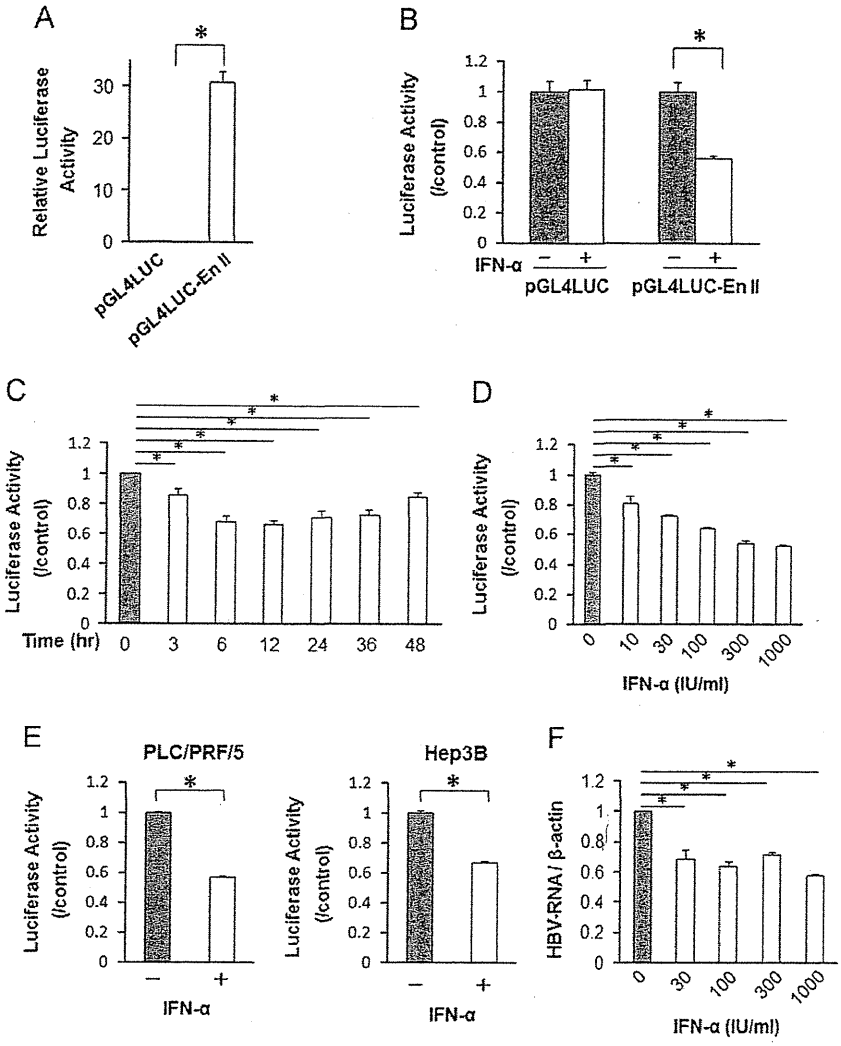

Fig. 2. Suppression of HBV En II transcriptional activity and reduction of HBV-RNA by IFN-α. A, B. Huh-7 cells were transfected with pGL4LUC or pGL4LUC-En II or incubated with or without IFN-α (100 IU/ml). After 24 h, the activity of firefly luciferase was evaluated. C. Huh-7 cells were transfected with pGL4LUC-En II, and incubated with IFN-α (100 IU/ml). Luciferase activities were evaluated at the indicated times. D. Huh-7 cells were transfected with various concentrations (0–1000 IU/ml) of IFN-α for 12 h and luciferase activities were evaluated. E. PLC/PRF/5 cells (left panel) and Hep3B (right panel) cells were transfected with pGL4LUC-En II, and incubated with or without IFN-α (300 IU/ml). Luciferase activities were evaluated. F. Huh-7 cells were transfected with pHBV1.5, and treated with IFN-α at various concentrations (0–1000 IU/ml). At 72 h after IFN-α treatment, cells were harvested, and the abundances of HBV-RNA were evaluated by quantitative RT-PCR. The HBV-RNA level of the IFN-α treated cells was normalized with that of non-treated cells. $*p < 0.05$. "/control" on the vertical axis means the ratio of luciferase activity of IFN-α treated cells normalized with that of non-treated cells.

not. Since staurosporine is a PKC inhibitor showing broad-spectrum activity (Marte et al., 1994), we also examined other inhibitors specific for PKC isoforms. Previous reports demonstrated that IFN-α activated PKC-α/β and PKC-δ (Pfeffer et al., 1990; Uddin et al., 2002). Indeed, activation of PKC-α/β and PKC-δ by IFN-α was confirmed by immunoblot analysis (Fig. 5B). Thus, we examined the PKC inhibitors rottlerin and Gö6976 (Gschwendt et al., 1994; Martiny-Baron et al., 1993). All PKC inhibitors blocked the suppression of En II activity by IFN-α (Fig. 5C). These results suggest that several isoforms of PKC are involved in the IFN-α-mediated suppression of En II activity. We also examined STAT1 activation and ISGs induction by IFN-α in cells pre-treated with these PKC inhibitors using immunoblot analysis (Fig. 5D). Expression levels of phospho-STAT1 and Mx differed among these PKC inhibitors. Staurosporine and Gö6976 slightly diminished the activation of STAT1, but rottlerin did not. This result suggests that PKC isoforms might not strongly regulate activation of STAT1. Rottlerin, a specific inhibitor for PKC-δ, inhibited the induction of Mx, which agreed with previous findings (Kaur et al., 2005). Staurosporine and Gö6976 did not suppress Mx expression. Taken together, all these PKC inhibitors blocked the suppression of En II activity by IFN-α regardless of the expression levels of phospho-STAT1 and Mx. These results suggest that STAT1 activation and ISG induction may be dispensable for the IFN-α-mediated suppression of En II activity. Next, we examined the effect of phorbol 12-myristate 13-acetate (PMA), a PKC activator (Castagna et al., 1982; Griner and Kazanietz, 2007). PMA suppressed En II activity (Fig. 5E), and PMA stimulation did not result in STAT1 phosphorylation and Mx induction (Fig. 5F), suggesting that suppression of En II by PMA is independent of STAT1 activation and ISG induction. On the basis of these findings, we conclude that IFN-α suppresses En II activity via the PKC pathway, which may not involve STAT1 activation and ISG induction.

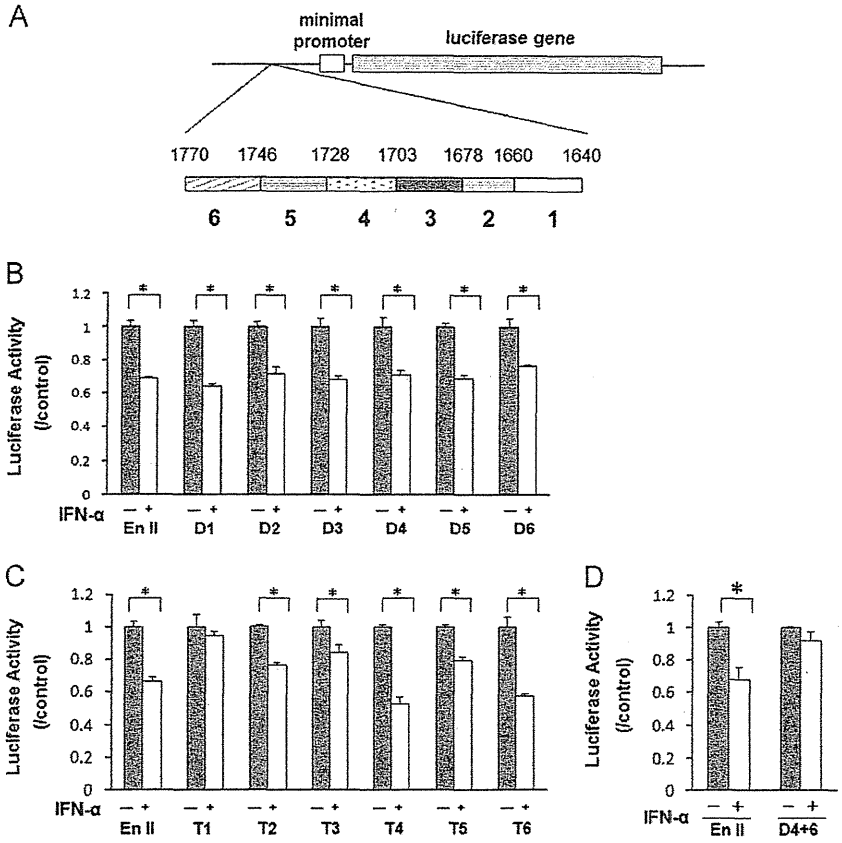

Fig. 3. Deletion/mutational analysis to identify the responsive sequence for the suppressive effect of IFN-α on En II. A. Scheme of pGL4LUC-En II and six segments defined within the En II sequence. The En II sequence was integrated just upstream of the minimal promoter of pGL4LUC. B. Huh-7 cells were transfected with the reporter vectors with deletion of each segment (pGL4LUC-En II-D1~6), incubated with 300 IU/ml IFN-α for 12 h, and luciferase activities were evaluated. C. Plasmids containing four iterations of each segment within En II sequence in tandem (pGL4LUC-En II-T1~6) were generated and luciferase activities were evaluated similarly. D. Plasmid with deletion of both nt 1703–1727 and nt 1746–1770 (pGL4LUC-En II-D4+6) was constructed and luciferase activities were evaluated similarly. $^*p < 0.05$. "/control" on the vertical axis means the ratio of luciferase activity of IFN-α treated cells normalized with that of non-treated cells.

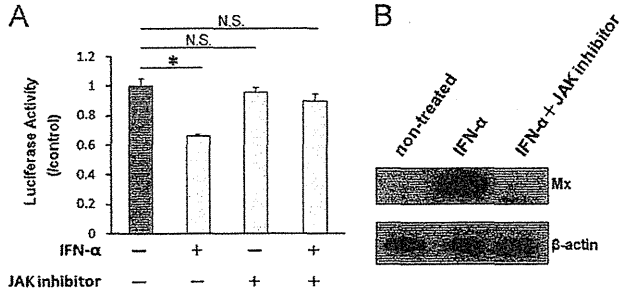

Fig. 4. Involvement of JAK activation in the IFN-α-induced suppression of En II activity. A. Huh-7 cells were transfected with pGL4LUC-En II and treated with JAK inhibitor (1 μM) for 1 h. The cells were then incubated with IFN-α(150 IU/ml) for 12 h, followed by luciferase assay. B. Huh-7 cells were pre-treated with JAK inhibitor for 1 h, and then incubated with IFN-α(150 IU/ml) for 12 h, followed by immunoblot analyses to detect Mx protein. $^*p < 0.05$. "/control" on the vertical axis means the ratio of luciferase activity of IFN-α treated cells normalized by that of non-treated cells.

Table 1
A comment of the inhibitors and its target kinase.

PD98059	MEK inhibitor
SB203580	P38MAPK inhibitor
LY294002	PI3K inhibitor
Akt-1-1/2	Akt inhibitor
SP600125	JNK inhibitor
Staurosporine	PKC inhibitor with broad spectrum
Rottlerin	Inhibitor specific for PKC-δ
G66976	Inhibitor specific for Ca^{2+}-dependent PKC isoforms

Knockdown of a single transcription factor does not influence IFN-α-induced suppression of En II activity

We anticipated that IFN-α suppressed En II activity by functional down-regulation of some transcription factor(s) phosphorylated in a PKC-dependent manner. Among transcription factors which bind the En II region, previous reports showed that Specificity Protein 1 (Sp1) (Mahoney et al., 1992; Pal et al., 1998; Rafty and Khachigian, 2001), Retinoid X Receptor α (RXRA) (Delmotte et al., 1999) and C/EBP (Mahoney et al., 1992) were inactivated by PKC. Thus, we examined the En II response to IFN-α after knockdown of these transcription factors. C/EBP, RXR and Sp1 expression was efficiently reduced by siRNA (Fig. 6A). We observed no significant change in the suppression of En II activity compared with control siRNA (Fig. 6B). This result suggests that several transcription factors (including unknown proteins) might be involved in the IFN-α-mediated suppression of En II activity.

Discussion

In the present study, we demonstrated that IFN-α suppressed HBV En II activity. The inhibition by IFN-α of En II activity could be blocked by pre-treatment with PKC inhibitors, and this

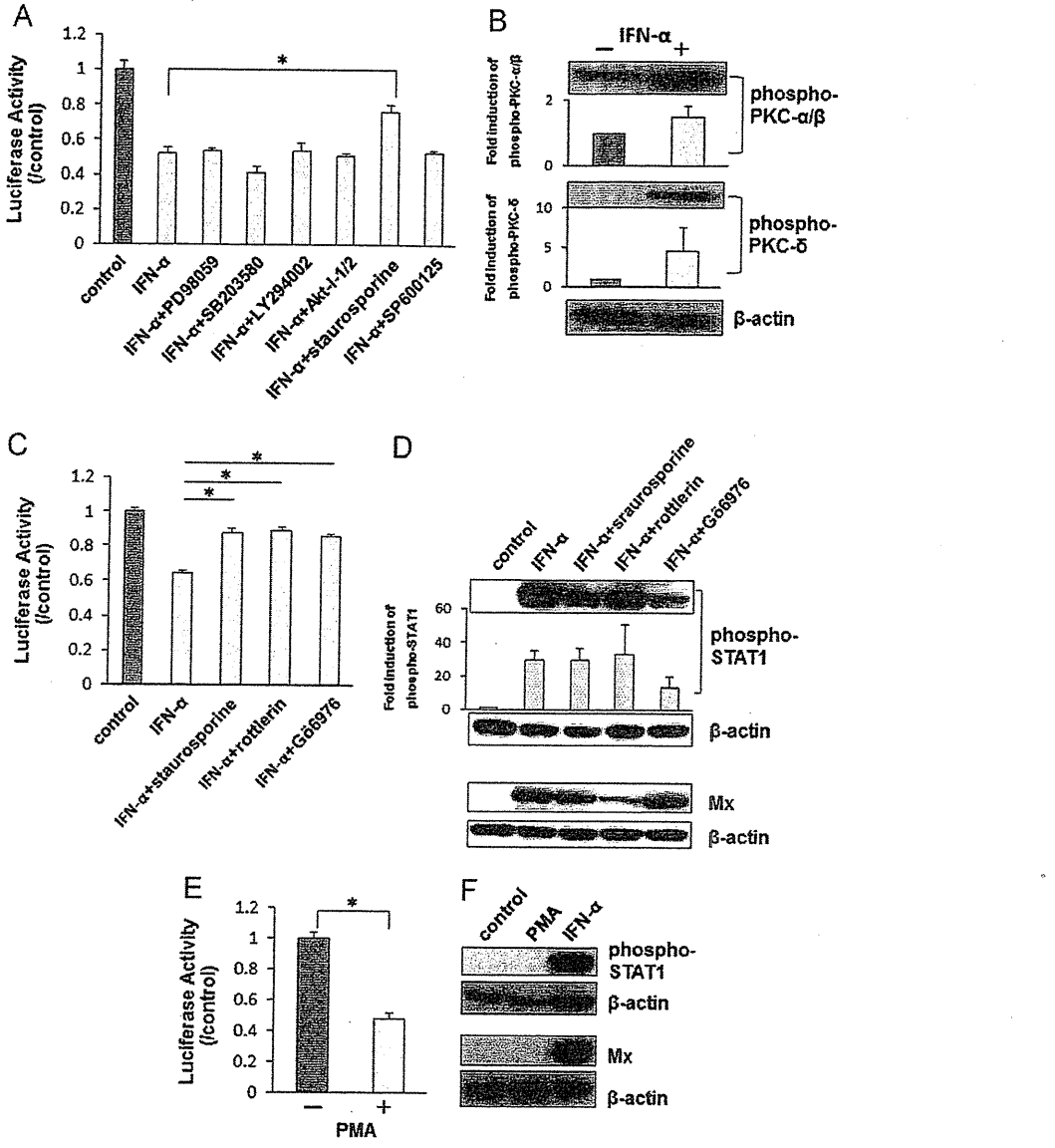

Fig. 5. PKC-dependent suppression of En II activity by IFN-α. A and C. Huh-7 cells were transfected with pGL4LUC-En II, treated separately with each kinase inhibitor for 1 h. The cells were then treated with IFN-α(1000 IU/ml) for 12 h, and luciferase activities were evaluated. B. Huh-7 cells were treated with IFN-α(1000 IU/m) for 12 h. Immunoblot analyses were performed to detect phosphorylated PKC-α/β and phosphorylated PKC-δ. Quantitative analysis of the expression level of phopho- PKC-α/β and -δ was performed by using ImageJ. Each level was normalized with that of IFN-α-non-treated cells. D. Huh-7 cells were harvested at 30 min to detect phosphorylated STAT1 and at 12 h to detect the expression of Mx after administration of IFN-α (1000 IU/m), and immunoblot analyses were performed. Quantitative analysis of the expression level of phopho-STAT1 was performed by using ImageJ. Each level was normalized with that of IFN-α-non-treated cells. E. Huh-7 cells were transfected with pGL4LUC-En II, treated with PMA (100 nM) for 12 h, and luciferase activities were evaluated. F. Huh-7 cells were treated with PMA (100 nM) or IFN-α(1000 IU/m). The cells were harvested at 30 min to detect phosphorylated STAT1 and at 12 h to detect the expression of Mx, and immunoblot analyses were performed. *$p < 0.05$. "/control" on the vertical axis means the ratio of luciferase activity of IFN-α/ PMA treated cells normalized with that of non-treated cells.

blocking effect may not involve STAT1 activation and ISG induction. The latter, ISG induction via the JAK-STAT pathway, has been considered to be the main mechanism suppressing viral replication. Our findings suggest a pathway for IFN-α repression of HBV transcription other than ISG induction.

PKCs are involved in a wide variety of cell functions and signal transduction pathways regulating cell migration and polarity, proliferation, differentiation and cell death (Nishizuka, 1988). In the PKC family, there are at least ten isoforms which can be divided into three sub-groups based on their structural characteristics and cofactor requirements. These include the classical PKC (cPKC: α, βI, βII, and γ), the novel PKC (nPKC: δ, ε, η and θ), and the atypical PKC (aPKC: ζ and ι/λ) (Azzi et al., 1992; Breitkreutz et al., 2007; Kikkawa et al., 1989). IFN-α can activate multiple PKC isoforms: not only PKC-δ, but also PKC-α/β (Pfeffer et al., 1990), PKC-ε (Pfeffer et al., 1991), and PKC-θ (Srivastava et al., 2004). Despite the variety of PKC isoforms, most phosphorylate similar sequences (Breitkreutz et al., 2007). Both the PKC-α/β inhibitor (Gö6976) and PKC-δ inhibitor (rottlerin) blocked the inhibitory effect of IFN-α on En II activity. Thus, it was speculated that each PKC isoform might be similarly involved in suppressing of En II activity.

Other studies have examined the role of the PKC pathway in HBV replication. Kang et al. (2008) reported that PKC-mediated phosphorylation increased capsid assembly and stability (von Hahn et al., 2011), and von Hahn et al. (2011) reported that the

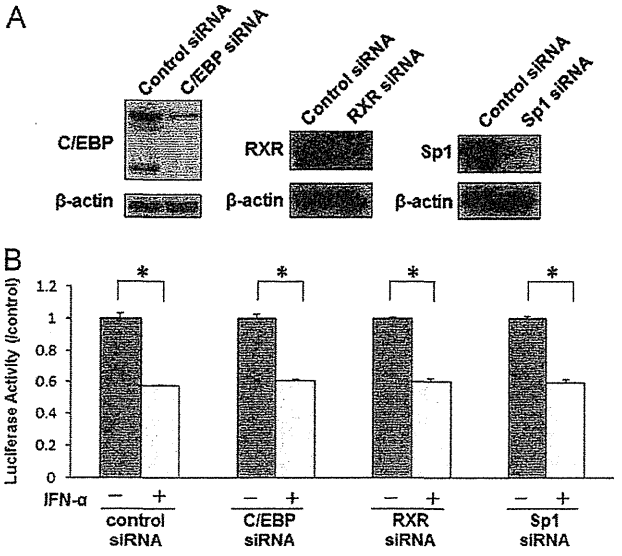

Fig. 6. IFN-α-mediated suppression on En II activity with knockdown of C/EBP, RXR and Sp1. A. Huh-7 cells were transfected with 10 nM siRNA (negative control or specific for C/EBP, RXR and Sp1). Immunoblot analyses for expressions of C/EBP, RXR, Sp1 and β-actin were performed at 48 h post siRNA transfection. B. Huh-7 cells were transfected with 10 nM siRNA (negative control or specific for C/EBP, RXR and Sp1). On the next day, si-RNA treated cells were transfected again with pGL4LUC-En II. On the following day, these transfected cells were incubated with IFN-α(1000 IU/ml) for 12 h, and luciferase activities were evaluated. "/control" on the vertical axis means the ratio of luciferase activity of IFN-α treated cells normalized with that of non-treated cells.

pan-PKC inhibitor sotrastaurin did not affect HBV replication. While the role of PKC in the HBV life cycle is still controversial, our findings suggest that PKC isoforms activated by IFN-α play inhibitory roles in HBV transcription by down-regulation of En II activity. As von Hahn et al. reported, sotrastaurin alone did not affect HBV replication. But, based on our present data about another pan-PKC inhibitor, staurosporine, we speculate that sotrastaurin may also block the inhibitory effect of IFN-α on En II activity.

We showed that knockdown of a single transcription factor did not influence the IFN-α-mediated suppression of En II activity, suggesting that several transcription factors might be involved in this suppression. We also showed that both segment 4 (nt 1703–1727) and segment 6 (nt 1746–1770) within the En II region are required for the IFN-α-induced suppression of En II activity. Although these two regions seem to be more important than the others, all the deleted version of reporter constructs showed almost completely similar suppression activities (Fig. 3B). We speculate that there may be some transcription factors which affect both the segment 4 and 6. Even if one of these regions is deleted, some factors may affect the other region, and result in the suppression of En II activity. Further study will be needed to clarify the mechanism.

Indeed, there are no identified transcription factors which could bind both segment 4 and 6. Only two transcription factors (HNF1 and 3) were reported to bind segment 4 (Johnson et al., 1995; Wang et al., 1998), and there have been no reports indicating that IFN-α or PKC inactivates HNF1 or 3. We also examined the expression levels of HNF1 and 3 of the IFN-α treated and the non-treated cells by RT-PCR. There was no significant difference in the expression of these transcription factors between the IFN-α treated and the non-treated cells (Nawa et al., unpublished data). Thus, we speculate that HNF1 or 3 might not be involved in the IFN-α mediated suppression of En II activity. There may be unknown transcription factors in the PKC pathway.

Previous reports showed that IFN-α suppressed En I activity (Nakao et al., 1999; Tur-Kaspa et al., 1990). Nakao et al. (1999) indicated that this occurred due to the binding of ISGF3 to an ISRE-like motif within the En I region. However, Rang et al. (2001) demonstrated that IFN-α reduced HBV-RNA levels derived from both HBV genome wild type and mutated ISRE-like motifs. This result contradicted the Nakao's result that the activity of the En I mutated ISRE-like motif was not suppressed by IFN-α. Schulte-Frohlinde et al. (2002) reported that IFN-α suppressed HBV core promoter regulated transcriptional activity, even when the ISRE-like motif of En I was deleted. The results of Rang et al. and Schulte-Frohlinde et al. suggest that IFN-α might suppress the activity of regions other than En I. In the present study, we demonstrated that IFN-α suppressed En II activity via the PKC pathway. En II might be one of the candidate regions down-regulated by IFN-α within the HBV genome.

Since En II activates viral transcription only in hepatocytes, it is responsible for the hepatocyte-specific gene expression of HBV. There had been no study on the effect of IFN-α on En II activity. Our study clarified that the PKC pathway is involved in the IFN-α-mediated suppression of En II activity, but may not involve ISG induction. Our result should aid in establishing better treatment with IFN-α against HBV infection. As we could not determine the molecule which inhibits En II activity by IFN-α, further study is needed to clarify this molecule and to control hepatitis B by IFN-α treatment.

Materials and methods

Plasmids

The HBV sequence used in this study was of the *adw2* subtype (GenBank accession no. X02763). Numbering of the HBV sequence started at the unique *Eco*RI site. The En II region in this study was defined as nt 1640–1771 of HBV sequence (Fig. 1) (Ishida et al., 2000). To construct pGL4LUC-En II, a plasmid containing the HBV En II region, the DNA fragment was amplified with PCR and inserted between *Hind* III and *Nhe* I site of pGL4 Luciferase Reporter Vector (pGL4LUC) (Promega, Madison, WI). The PCR primers were as follows: 5′-CCAAGCTTCTGCCCAAGGTC-3′ and 5′-CCCGCTAGCAAAGACCTTTAACCTAATCTCCTCC-3′. The constructs of the En II sequence with various deletions were generated by modifying pGL4LUC-En II using the QuikChange Site-Directed Mutagenesis Kit (Stratagene, La Jolla, CA). The constructs containing four tandem repeats of short fragment in En II sequence were generated by inserting duplexes of synthesized oligonucleotides into the multi-cloning site of pGL4LUC. All of the En II sequences were inserted in the antisense orientation to evaluate their enhancer activity.

Plasmid pHBV1.5 containing a 1.5-fold-overlength genome of HBV-DNA (GenBank accession no. AF305422) has been described previously (Bruss and Ganem, 1991).

Cell lines and reagents

The human hepatocellular carcinoma cell lines Huh-7, PLC/PRF/5, and Hep3B were cultured in Dulbecco's modified Eagle's medium (DMEM) supplemented with 10% heat-inactivated fetal bovine serum (Sigma-Aldrich, St. Louis, MO) in a humidified incubator at 5% CO_2 and 37 °C. Human natural IFN-α was kindly provided by Hayashibara Biochemical Laboratories, Inc. (Okayama, Japan).

The inhibitors/activators and the final concentrations used were: JAK inhibitor I (1 μM), PD98059 (10 μM), SB203580 (10 μM), LY294002 (10 μM), Akt-I-1/2 (5 μM), staurosporine (10 or 20 nM), rottlerin (5 μM), Gö6976 (1 μM), SP600125 (10 μM)

(Calbiochem, San Diego, CA), phorbol 12-myristate 13-acetate (PMA) (100 nM) (Sigma-Aldrich, St. Louis, MO).

Plasmid transfection and luciferase assay

Huh-7 cells were co-transfected with the firefly luciferase plasmid and pGL4-RL-tk, an expression vector of renilla luciferase, which was used as an internal control, using FuGENE HD reagent (Roche Applied Science, Indianapolis, IN) according to the manufacturer's protocol. Activities of firefly luciferase and renilla luciferase were measured using the Dual-Glo Luciferase Assay System (Promega, Madison, WI), and then relative luciferase activity was calculated by normalizing firefly luciferase activity to renilla luciferase activity.

RNA extraction

Total RNA was isolated from cells using ISOGEN (Nippon Gene, Tokyo, Japan) according to the manufacturer's protocol. The isolated RNA was treated with DNase I (Promega, Madison, WI) to avoid contamination with transfected plasmid, and then purified with a mixture of phenol, chloroform, and isoamylalcohol (pH 7.9), followed by ethanol precipitation.

Western blot analysis

Cultured cells were lysed with a lysis buffer (1% NP-40, 0.5% sodium deoxycholate, 0.1% SDS, and protein inhibitor cocktail (Nacalai Tesque), in PBS, pH 7.4). Equal amounts of protein were electrophoretically separated by polyacrylamide gel and transferred onto PVDF membrane. For immunodetection, the following antibodies were used: anti-STAT1 antibody, anti-phospho-STAT1 antibody, anti-phospho-PKC-α/β II (Thr 638/641) antibody, anti-phospho-PKC-δ (Thr 505) antibody, anti-C/EBP antibody, anti-RXR antibody, anti-Sp1 antibody, anti-β-actin antibody from Cell Signaling Technology (Beverly, MA), and anti-Mx antibody from Abcam (Cambridge, UK). The signals of phosphorlylated proteins such as phospho-PKC-α/β, -δ and phospho-STAT1 were analyzed quantitatively using image analyzing software (ImageJ; version 1.45).

Small RNA interference

Stealth Select RNAi specific for STAT1 (HSS 10273) was purchased from Invitrogen (Carlsbad, CA). Silencer Select siRNA specific for C/EBP (ID: S2890), RXR (ID: S12386) and Sp1 (ID: S13319) were purchased from Ambion (Austin, TX). Stealth RNAi Negative Control Low GC Duplex (Invitrogen, Carlsbad, CA) was used as a control for the off-target effect following Stealth Select RNAi delivery. The transfections were carried out using Lipofectamine RNAiMAX (Invitrogen, Carlsbad, CA) according to the reverse transfection protocol.

Real-time reverse-transcription PCR

For cDNA synthesis, 1 μg of total RNA was reverse-transcribed using High Capacity RNA-to-DNA Master Mix (Applied Biosystems, Foster City, CA). cDNA, equivalent to 20 ng RNA, was used as a template for real-time reverse-transcription PCR (RT-PCR) using Applied Biosystems 7900HT Fast Real-Time PCR System (Applied Biosystems, Foster City, CA). mRNA expressions of C/EBP, FTF, HNF1, HNF3, and HNF4 were measured using TaqMan Gene Expression Assays and were corrected with the quantified expressions level of β-actin mRNA. Assay IDs for the genes were as follows: C/EBP (Hs00269972_s1), FTF (Hs00187067_m1), HNF1 (Hs00167041_m1), HNF3 (Hs00232754_m1), and HNF4 (Hs01023298_m1).

For the detection of pgRNA and pre-C mRNA, the primers and the probes were designed as follows according to a previous study (Laras et al., 2002): the sense primer was 5′-TCTTGTACATGTCCCACTGTTCAA-3′ (nt 1843–1866); the anti-sense primer was 5′-AATGCCATGCCCCAAAGC-3′ (nt 1890–1909); the probe was 5′-FAM-CTCCAAGCTGTGCCTT-3′ (nt 1869–1884). Since they were within precore/core coding sequence, only the total abundance of pgRNA and pre-C RNA could be detected.

Statistical analysis

Data were presented as mean ± SD. Differences between two groups were determined using Student's t-test for unpaired observations. $p < 0.05$ was considered statistically significant.

Disclosures

All authors have nothing to disclose.

References

Antonucci, T.K., Rutter, W.J., 1989. Hepatitis B virus (HBV) promoters are regulated by the HBV enhancer in a tissue-specific manner. J. Virol. 63, 579–583.

Azzi, A., Boscoboinik, D., Hensey, C., 1992. The protein kinase C family. Eur. J. Biochem. 208, 547–557.

Beck, J., Nassal, M., 2007. Hepatitis B virus replication. World J. Gastroenterol. 13, 48–64.

Breitkreutz, D., Braiman-Wiksman, L., Daum, N., Denning, M.F., Tennenbaum, T., 2007. Protein kinase C family: on the crossroads of cell signaling in skin and tumor epithelium. J. Cancer Res. Clin. Oncol. 133, 793–808.

Bruss, V., Ganem, D., 1991. The role of envelope proteins in hepatitis B virus assembly. Proc. Nat. Acad. Sci. U.S.A. 88, 1059–1063.

Caraglia, M., Abbruzzese, A., Leardi, A., Pepe, S., Budillon, A., Baldassare, G., Selleri, C., Lorenzo, S.D., Fabbrocini, A., Giuberti, G., Vitale, G., Lupoli, G., Bianco, A.R., Tagliaferri, P., 1999. Interferon-alpha induces apoptosis in human KB cells through a stress-dependent mitogen activated protein kinase pathway that is antagonized by epidermal growth factor. Cell Death Differ. 6, 773–780.

Castagna, M., Takai, Y., Kaibuchi, K., Sano, K., Kikkawa, U., Nishizuka, Y., 1982. Direct activation of calcium-activated, phospholipid-dependent protein kinase by tumor-promoting phorbol esters. J. Biol. Chem. 257, 7847–7851.

Darnell, J.E., Kerr, I.M., Stark, G.R., 1994. Jak-STAT pathways and transcriptional activation in response to IFNs and other extracellular signaling proteins. Science 264, 1415–1421.

David, M., Petricoin, E., Benjamin, C., Pine, R., Weber, M.J., Larner, A.C., 1995. Requirement for MAP kinase (ERK2) activity in interferon alpha- and interferon beta-stimulated gene expression through STAT proteins. Science 269, 1721–1723.

Delmotte, M.H., Tahayato, A., Formstecher, P., Lefebvre, P., 1999. Serine 157, a retinoic acid receptor alpha residue phosphorylated by protein kinase C in vitro, is involved in RXR.RARalpha heterodimerization and transcriptional activity. J. Biol. Chem. 274, 38225–38231.

Der, S.D., Zhou, A., Williams, B.R., Silverman, R.H., 1998. Identification of genes differentially regulated by interferon alpha, beta, or gamma using oligonucleotide arrays. Proc. Nat. Acad. Sci. U.S.A. 95, 15623–15628.

Goh, K.C., Haque, S.J., Williams, B.R., 1999. p38 MAP kinase is required for STAT1 serine phosphorylation and transcriptional activation induced by interferons. EMBO J. 18, 5601–5608.

Griner, E.M., Kazanietz, M.G., 2007. Protein kinase C and other diacylglycerol effectors in cancer. Nat. Rev. Cancer 7, 281–294.

Gschwendt, M., Müller, H.J., Kielbassa, K., Zang, R., Kittstein, W., Rincke, G., Marks, F., 1994. Rottlerin, a novel protein kinase inhibitor. Biochem. Biophys. Res. Commun. 199, 93–98.

Guo, W., Chen, M., Yen, T.S., Ou, J.H., 1993. Hepatocyte-specific expression of the hepatitis B virus core promoter depends on both positive and negative regulation. Mol. Cell. Biol. 13, 443–448.

Ishida, H., Ueda, K., Ohkawa, K., Kanazawa, Y., Hosui, A., Nakanishi, F., Mita, E., Kasahara, A., Sasaki, Y., Hori, M., Hayashi, N., 2000. Identification of multiple transcription factors, HLF, FTF, and E4BP4, controlling hepatitis B virus enhancer II. J. Virol. 74, 1241–1251.

Johnson, J.L., Raney, A.K., McLachlan, A., 1995. Characterization of a functional hepatocyte nuclear factor 3 binding site in the hepatitis B virus nucleocapsid promoter. Virology 208, 147–158.

Jonas, M.M., Block, J.M., Haber, B.A., Karpen, S.J., London, W.T., Murray, K.F., Narkewicz, M.R., Rosenthal, P., Schwarz, K.B., McMahon, B.J., Foundation, H.B., 2010. Treatment of children with chronic hepatitis B virus infection in the United States: patient selection and therapeutic options. Hepatology 52, 2192–2205.

Kang, H., Yu, J., Jung, G., 2008. Phosphorylation of hepatitis B virus core C-terminally truncated protein (Cp149) by PKC increases capsid assembly and stability. Biochem. J. 416, 47–54.
Kaur, S., Parmar, S., Smith, J., Katsoulidis, E., Li, Y., Sassano, A., Majchrzak, B., Uddin, S., Tallman, M.S., Fish, E.N., Platanias, L.C., 2005. Role of protein kinase C-delta (PKC-delta) in the generation of the effects of IFN-alpha in chronic myelogenous leukemia cells. Exp. Hematol. 33, 550–557.
Kikkawa, U., Kishimoto, A., Nishizuka, Y., 1989. The protein kinase C family: heterogeneity and its implications. Annu. Rev. Biochem. 58, 31–44.
Laras, A., Koskinas, J., Hadziyannis, S.J., 2002. In vivo suppression of precore mRNA synthesis is associated with mutations in the hepatitis B virus core promoter. Virology 295, 86–96.
Li, M., Xie, Y., Wu, X., Kong, Y., Wang, Y., 1995. HNF3 binds and activates the second enhancer, ENII, of hepatitis B virus. Virology 214, 371–378.
Li, M., Xie, Y.H., Kong, Y.Y., Wu, X., Zhu, L, Wang, Y., 1998. Cloning and characterization of a novel human hepatocyte transcription factor, hB1F, which binds and activates enhancer II of hepatitis B virus. J. Biol. Chem. 273, 29022–29031.
Liaw, Y.F., 2009. HBeAg seroconversion as an important end point in the treatment of chronic hepatitis B. Hepatol. Int.
Lok, A.S., McMahon, B.J., 2009. Chronic hepatitis B: update 2009. Hepatology 50, 661–662.
López-Cabrera, M., Letovsky, J., Hu, K.Q., Siddiqui, A., 1990. Multiple liver-specific factors bind to the hepatitis B virus core/pregenomic promoter: trans-activation and repression by CCAAT/enhancer binding protein. Proc. Nat. Acad. Sci. U.S.A. 87, 5069–5073.
López-Cabrera, M., Letovsky, J., Hu, K.Q., Siddiqui, A., 1991. Transcriptional factor C/EBP binds to and transactivates the enhancer element II of the hepatitis B virus. Virology 183, 825–829.
Mahoney, C.W., Shuman, J., McKnight, S.L., Chen, H.C., Huang, K.P., 1992. Phosphorylation of CCAAT-enhancer binding protein by protein kinase C attenuates site-selective DNA binding. J. Biol. Chem. 267, 19396–19403.
Marte, B.M., Meyer, T., Stabel, S., Standke, G.J., Jaken, S., Fabbro, D., Hynes, N.E., 1994. Protein kinase C and mammary cell differentiation: involvement of protein kinase C alpha in the induction of beta-casein expression. Cell Growth Differ. 5, 239–247.
Martiny-Baron, G., Kazanietz, M.G., Mischak, H., Blumberg, P.M., Kochs, G., Hug, H., Marmé, D., Schächtele, C., 1993. Selective inhibition of protein kinase C isozymes by the indolocarbazole Gö 6976. J. Biol. Chem. 268, 9194–9197.
Moolla, N., Kew, M., Arbuthnot, P., 2002. Regulatory elements of hepatitis B virus transcription. J. Viral. Hepat. 9, 323–331.
Nakao, K., Nakata, K., Yamashita, M., Tamada, Y., Hamasaki, K., Ishikawa, H., Kato, Y., Eguchi, K., Ishii, N., 1999. p48 (ISGF-3gamma) is involved in interferon-alpha-induced suppression of hepatitis B virus enhancer-1 activity. J. Biol. Chem. 274, 28075–28078.
Nishizuka, Y., 1988. The molecular heterogeneity of protein kinase C and its implications for cellular regulation. Nature 334, 661–665.
Pal, S., Claffey, K.P., Cohen, H.T., Mukhopadhyay, D., 1998. Activation of Sp1-mediated vascular permeability factor/vascular endothelial growth factor transcription requires specific interaction with protein kinase C zeta. J. Biol. Chem. 273, 26277–26280.
Pfeffer, L.M., Eisenkraft, B.L., Reich, N.C., Improta, T., Baxter, G., Daniel-Issakani, S., Strulovici, B., 1991. Transmembrane signaling by interferon alpha involves diacylglycerol production and activation of the epsilon isoform of protein kinase C in Daudi cells. Proc. Nat. Acad. Sci. U.S.A. 88, 7988–7992.
Pfeffer, L.M., Strulovici, B., Saltiel, A.R., 1990. Interferon-alpha selectively activates the beta isoform of protein kinase C through phosphatidylcholine hydrolysis. Proc. Nat. Acad. Sci. U.S.A. 87, 6537–6541.
Rafty, L.A., Khachigian, L.M., 2001. Sp1 phosphorylation regulates inducible expression of platelet-derived growth factor B-chain gene via atypical protein kinase C-zeta. Nucleic Acids Res. 29, 1027–1033.
Raney, A.K., Johnson, J.L., Palmer, C.N., McLachlan, A., 1997. Members of the nuclear receptor superfamily regulate transcription from the hepatitis B virus nucleocapsid promoter. J. Virol. 71, 1058–1071.
Rang, A., Heise, T., Will, H., 2001. Lack of a role of the interferon-stimulated response element-like region in interferon alpha -induced suppression of Hepatitis B virus in vitro. J. Biol. Chem. 276, 3531–3535.
Romero, R., Lavine, J.E., 1996. Cytokine inhibition of the hepatitis B virus core promoter. Hepatology 23, 17–23.
Schulte-Frohlinde, E., Seidler, B., Burkard, I., Freilinger, T., Lersch, C., Erfle, V., Foster, G.R., Classen, M., 2002. Different activities of type I interferons on hepatitis B virus core promoter regulated transcription. Cytokine 17, 214–220.
Srivastava, K.K., Batra, S., Sassano, A., Li, Y., Majchrzak, B., Kiyokawa, H., Altman, A., Fish, E.N., Platanias, L.C., 2004. Engagement of protein kinase C-theta in interferon signaling in T-cells. J. Biol. Chem. 279, 29911–29920.
Su, H., Yee, J.K., 1992. Regulation of hepatitis B virus gene expression by its two enhancers. Proc. Nat. Acad. Sci. U.S.A. 89, 2708–2712.
Sureau, C., Romet-Lemonne, J.L., Mullins, J.I., Essex, M., 1986. Production of hepatitis B virus by a differentiated human hepatoma cell line after transfection with cloned circular HBV DNA. Cell 47, 37–47.
Tur-Kaspa, R., Teicher, L., Laub, O., Itin, A., Dagan, D., Bloom, B.R., Shafritz, D.A., 1990. Alpha interferon suppresses hepatitis B virus enhancer activity and reduces viral gene transcription. J. Virol. 64, 1821–1824.
Uddin, S., Sassano, A., Deb, D.K., Verma, A., Majchrzak, B., Rahman, A., Malik, A.B., Fish, E.N., Platanias, L.C., 2002. Protein kinase C-delta (PKC-delta) is activated by type I interferons and mediates phosphorylation of Stat1 on serine 727. J. Biol. Chem. 277, 14408–14416.
Uddin, S., Yenush, L., Sun, X.J., Sweet, M.E., White, M.F., Platanias, L.C., 1995. Interferon-alpha engages the insulin receptor substrate-1 to associate with the phosphatidylinositol 3'-kinase. J. Biol. Chem. 270, 15938–15941.
Vannice, J.L., Levinson, A.D., 1988. Properties of the human hepatitis B virus enhancer: position effects and cell-type nonspecificity. J. Virol. 62, 1305–1313.
von Hahn, T., Schulze, A., Chicano Wust, I., Heidrich, B., Becker, T., Steinmann, E., Helfritz, F.A., Rohrmann, K., Urban, S., Manns, M.P., Pietschmann, T., Ciesek, S., 2011. The novel immunosuppressive protein kinase C inhibitor sotrastaurin has no pro-viral effects on the replication cycle of hepatitis B or C virus. PLoS One 6, e24142.
Wang, W.X., Li, M., Wu, X., Wang, Y., Li, Z.P., 1998. HNF1 is critical for the liver-specific function of HBV enhancer II. Res. Virol. 149, 99–108.
Wang, Y., Chen, P., Wu, X., Sun, A.L., Wang, H., Zhu, Y.A., Li, Z.P., 1990. A new enhancer element, ENII, identified in the X gene of hepatitis B virus. J. Virol. 64, 3977–3981.
Yee, J.K., 1989. A liver-specific enhancer in the core promoter region of human hepatitis B virus. Science 246, 658–661.
Yuh, C.H., Ting, L.P., 1990. The genome of hepatitis B virus contains a second enhancer: cooperation of two elements within this enhancer is required for its function. J. Virol. 64, 4281–4287.
Yuh, C.H., Ting, L.P., 1991. C/EBP-like proteins binding to the functional box-alpha and box-beta of the second enhancer of hepatitis B virus. Mol. Cell. Biol. 11, 5044–5052.

IJC
International Journal of Cancer

Comparative analyses of regulatory T cell subsets in patients with hepatocellular carcinoma: A crucial role of $CD25^{-}FOXP3^{-}$ T cells

Naruyasu Kakita[1], Tatsuya Kanto[1,2], Ichiyo Itose[3], Shoko Kuroda[1], Michiyo Inoue[1], Tokuhiro Matsubara[1], Koyo Higashitani[1], Masanori Miyazaki[1], Mitsuru Sakakibara[1], Naoki Hiramatsu[1], Tetsuo Takehara[1], Akinori Kasahara[4] and Norio Hayashi[3]

[1] Department of Gastroenterology and Hepatology, Osaka University Graduate School of Medicine, Suita, Japan
[2] Department of Dendritic cell Biology and Clinical Applications, Osaka University Graduate School of Medicine, Suita, Japan
[3] Kansai Rosai Hospital, Amagasaki, Japan
[4] Department of General Medicine, Osaka University Hospital, Suita, Japan

Regulatory T cells (Tregs) play pivotal role in cancer-induced immunoediting. Increment of $CD25^{high+}FOXP3^{+}$ natural Tregs has been reported in patients with hepatocellular carcinoma (HCC); however, the involvement of other type of Tregs remain elusive. We aimed to clarify whether $FOXP3^{-}$ Tregs are increased and functionally suppressive or not in patients with HCC. We enrolled 184 hepatitis C-infected patients with chronic liver diseases or HCC, 57 healthy subjects and 27 HCC patients with other etiology. Distinct Treg subsets were phenotypically identified by the expression of CD4, CD25, CD127 and forkhead/winged helix transcription factor (FOXP3). Their gene profiles, frequency and suppressor functions against T cell proliferation were compared among the subjects. To examine the molecules involving in Treg differentiation, we cultured naive $CD4^{+}$ T cells in the presence of HCC cells and dendritic cells. We determined two types of $CD4^{+}CD127^{-}$ T cells with comparable regulatory ability; one is $CD25^{high+}$ cells expressing FOXP3 ($CD25^{high+}FOXP3^{+}$ Tregs) and the other is $CD25^{-}$ cells without $FOXP3^{-}$ expression ($CD25^{-}FOXP3^{-}$ cells). The peripheral or intrahepatic frequency of $CD25^{-}FOXP3^{-}$ Tregs in HCC patients is higher than those in other groups, of which significance is more than $CD25^{high+}FOXP3^{+}$ cells. Of importance, $CD25^{-}FOXP3^{-}$ Tregs, but not $CD25^{high+}FOXP3^{+}$ cells, dynamically change in patients accompanied by the ablation or the recurrence of HCC. $CD25^{-}FOXP3^{-}$ T cells with $CD127^{-}IL\text{-}10^{+}$ phenotype are inducible *in vitro* from naive $CD4^{+}$ T cells, in which programmed cell death 1 ligand 1, immunoglobulin-like transcript 4 and human leukocyte antigen G are involved.. In conclusion, $CD25^{-}FOXP3^{-}$ Tregs with suppressive capacity are increased in patients with HCC, suggesting their distinct roles from $CD25^{+}FOXP3^{+}$ Tregs.

Hepatocellular carcinoma (HCC) is the fifth most common cancer and the third leading cause of cancer-related deaths in the world.[1] One of the most prevalent risk factors for HCC is hepatotropic viruses, such as hepatitis B (HBV) or C (HCV) virus.[2,3] In the process of HCC development, the involvement of tumor-induced immune suppression; *i.e.*, immunoediting, has been implicated. Regulatory T cells (Tregs) are unique subset of T cells, playing essential roles in the maintenance of immune homeostasis or in the protection of hosts from virulent infections and cancers.[4] Generally, the existence of two types of Tregs has been reported. One is naturally occurring $CD4^{+}CD25^{high+}$ Tregs, which are derived from the thymus and suppress auto-reactive T cells. The other is inducible or adaptive Tregs, including interleukin (IL)-10-secreting type-1 regulatory T cells (Tr1) and transforming growth factor (TGF)-β-producing Th3. These are inducible in the

Key words: HCC, regulatory T cells, FOXP3, CD25, CD127

Abbreviations: CTLA-4: cytotoxic T-lymphocyte antigen 4; DC: dendritic cell; FOXP3: forkhead/winged helix transcription factor; GITR: glucocorticoid-induced TNF receptor family-regulated gene; HBV: hepatitis B virus; HCC: hepatocellular carcinoma; HCV: hepatitis C virus; IL-T4: immunoglobulin-like transcript 4; LAG-3: lymphocyte-activation gene 3; PBMC: peripheral blood mononuclear cell; PD-1: programmed cell death 1; PD-L1: programmed cell death 1 ligand 1; RFA: radiofrequency ablation; RT-PCR: reverse transcription polymerase chain reaction; Tr1: type-1 regulatory T cells; Tregs: regulatory T cells

Additional Supporting Information may be found in the online version of this article.

Grant sponsors: Grant-In-Aid for Scientific Research from the Ministry of Education, Culture, Sports, Science and Technology of Japan, a Grant-in-Aid from the Ministry of Health, Labour and Welfare of Japan

DOI: 10.1002/ijc.27535

History: Received 23 Jul 2011; Accepted 28 Feb 2012; Online 15 Mar 2012

Correspondence to: Tatsuya Kanto, Department of Gastroenterology and Hepatology, Osaka University Graduate School of Medicine, 2-2 Yamadaoka, Suita 565-0871 Japan, Tel: +81-6-6879-3621, Fax: +81-6-6879-3629, E-mail: kantot@gh.med.osaka-u.ac.jp

Table 1. Clinical backgrounds of the patients enrolled in the study[1]

	HV	CH (C)	LC (C)	HCC (C)	HCC (B)	HCC (NBNC)
N	57	66	39	79	12	15
Gender (M/F)	35/22	44/22	23/16	44/35	8/4	9/6
Age (years)	56 ± 11	56 ± 18	61 ± 9	66 ± 11	56 ± 9	62 ± 13
ALT (IU/l)	ND	70 ± 15	44 ± 13	56 ± 17	65 ± 7	45 ± 11
Platelets ($10^4/\mu l$)	ND	15 ± 4	11 ± 4	12 ± 4	13 ± 4	12 ± 4
Total bilirubin (mg/ml)	ND	0.9 ± 0.4	1.6 ± 0.4[2]	0.9 ± 0.3	0.6 ± 0.1	0.7 ± 0.3
Alb (g/dl)	ND	3.7 ± 0.5	3.3 ± 0.4	3.1 ± 0.6[2]	3.5 ± 0.2	3.6 ± 0.3
AFP (ng/ml)[3]	ND	2-115 (15)	2-347 (16)	4-33357 (43)	7-12 (10)	10-16520 (23)
TNM stage[4] (I + II/III + IV)	–	–	–	55/24	9/3	9/6

[1]All values except for AFP are expressed as mean ± standard deviation. [2]$p < 0.05$ *vs.* CH (C) group. [3]Values are expressed as range (median).
[4]Seventh edition of International Union Against Cancer TNM staging system of HCC.
Abbreviations: HV, healthy volunteers; CH (C), LC (C), HCC (C), HCV-positive chronic hepatitis, liver cirrhosis and hepatocellular carcinoma; HCC (B), HBV-positive hepatocellular carcinoma; HCC (NBNC), non-B, non-C hepatocellular carcinoma; ALT, alanine aminotransferase; Alb, albumin; AFP, alfa-fetoprotein; ND, not determined.

periphery and are endowed with the ability to suppress antigen-specific T cells.[5] Several reports have shown that natural Tregs are increased in peripheral blood and/or tumor in patients with various types of cancer.[6] In HBV-infected HCC patients, an increase in natural Tregs and their suppressor functions against antigen-specific CTLs has been reported.[7] A correlation has been observed between natural Treg frequency and recurrence-free or overall survival of HCC patients.[8] However, it is yet to be determined if a distinct Treg subset is involved or not in the development of HCC.

The forkhead/winged helix transcription factor, FOXP3, is acknowledged as a major and specific marker of Tregs, the cellular expression of which is correlated with suppressive activities.[9] However, in the differentiation from naive T cells to effector/memory T cells, FOXP3 is transiently expressed but not sustained, suggesting that some proportion of $FOXP3^+$ T cells are not regulatory but activated ones.[10] These observations suggest that using FOXP3 as a marker of functionally regulatory cells would be limited and not suitable for adaptive Tregs. In recent studies, the expression of IL-7 receptor alpha chain (CD127) was found to be downregulated in Tregs and CD127 expression to be inversely correlated with FOXP3 expression.[11,12] Moreover, CD127-negative T cells are endowed with suppressive ability irrespective of their CD25 expression.[13] Alternatively, several studies have shown that CD127 is downregulated on $FOXP3^-$ Tr1 cells.[14,15] Due to the lack of specific or appropriate markers for identification of adaptive Tregs, it is yet to be confirmed that $FOXP3^-$ T cells are adaptive Tregs. Furthermore, little is known about the precise roles of $FOXP3^-$ regulatory cells in the development of HCC.

In this study, we focused on $FOXP3^-$ Tregs and tried to elucidate whether or not such cells are associated with the presence of HCC. To assess the feasibility of $FOXP3^-$ cells as a therapeutic target for immunological control of HCC, we tried to clarify the molecular mechanisms of its induction.

Material and Methods

Subjects

Among chronically HCV-infected patients who had been followed at Osaka University Hospital, we enrolled 184 patients who were further categorized into three groups according to the stages of liver disease: chronic hepatitis (CH), liver cirrhosis (LC) and HCC groups. The clinical stage of HCC was determined according to the TNM classification system of the International Union against Cancer (seventh edition). The study protocol was approved by the ethical committee at the Osaka University Graduate School of Medicine. At enrollment, written informed consent was obtained from all patients and volunteers. Some of HCC patients in this study received radiofrequency ablation (RFA) therapy. Indication for RFA therapy was based on therapeutic guidelines for HCC promoted by the Japan Society of Hepatology.[16] After the RFA session, the efficacy of tumor ablation or HCC recurrence thereafter was evaluated by computed tomography or magnetic resonance imaging scanning. In some of the HCC patients who underwent surgical resection, cancerous and adjacent noncancerous tissues were obtained at operation for further Treg analyses. As controls, 57 healthy subjects (HS) without history of liver diseases, 27 HCC patients with HBV infection (HBV-HCC group), those without HBV and HCV (non-B-, non-C [NBNC]-HCC group). The clinical backgrounds of the subjects are shown in Table 1.

Frequency analyses of peripheral and liver-infiltrating Tregs

Peripheral blood mononuclear cells (PBMCs) were stained with a combination of various fluorescence-labeled anti-human mouse or rat monoclonal antibodies (mAbs) as reported previously (17). The mAbs for CD4, CD25, CD127, FOXP3 and IL-10 were purchased from Becton Dickinson Biosciences (San Jose, CA). Fresh liver specimens were

washed twice with phosphate-buffered saline and were diced into 0.5 mm pieces. After these pieces were passed through a nylon mesh, liver-infiltrating lymphocytes were isolated by Ficoll-Hypaque density gradient centrifugation. These cells were stained with fluorescence-labeled Abs as performed for PBMC. For the analyses of FOXP3 and IL-10, we performed intracellular staining using a human FOXP3 staining kit (BD Biosciences) according to the manufacturer's instructions. The stained cells from PBMC or liver were analyzed by FACS Canto (BD Biosciences) and Cell Quest software.

Functional analysis of regulatory T cell subsets

To obtain live Tregs for functional analyses, we collected four populations of $CD4^+$ T cells according to the patterns of CD25 and CD127 expressions by FACS Aria (BD Biosciences). We cocultured various numbers of sorted cells with 1×10^5 allogenic naive $CD4^+CD25^-$ T cells in the presence of agonistic anti-CD3 and anti-CD28 Abs (BD Biosciences Pharmingen) on 96-well flat-bottom plates (Corning, Corning, NY) for 5 days. The proliferation of cells was assessed by incorporation of [3H]-thymidine. To clarify the suppression mechanism by Tregs, the cells were cultured with or without separation by transwell inserts (pore size 0.4 μm, Corning). Alternatively in some experiments, the cells were cultured in the presence or absence of neutralizing 10 ng/ml anti-IL-10 or anti-TGF-β Abs (R&D Systems, Mckinley, MN) or isotype IgG.

To examine regulatory cells possess suppressive function on recall antigen-specific $CD4^+$ T cell responses, we cocultured 1×10^4 each of sorted cells from some HCC patients with 1×10^5 autologous $CD4^+$ T cells in the presence or absence of 20 μg/ml of tetanus toxoid (Sigma) for 5 days, stimulated with 10 IU/ml of recombinant human IL-2 (BD Pharmingen). The proliferation of cells was assessed using WST-8 (2-(2-methoxy-4-nitrophenyl)-3-(4-nitrophenyl) -5 -(2,4-disulfophenyl)-2H-tetrazolium, monosodium salt) reagent in the Cell Counting Kit-8 (Dojindo, Japan) according to the manufacturer's instructions.

Real-time RT-PCR

To analyze gene profiles of Tregs, we collected $CD4^+CD25^{high+}CD127^-$ and $CD4^+CD25^-CD127^-$ T cells using FACS Aria. Extraction of total RNA and subsequent real-time reverse transcription polymerase chain reaction (RT-PCR) was performed as reported previously with some modifications.[17] Assays-on-demand primers and probes (Applied Biosystems, Foster City, CA) were used to quantify FOXP3, cytotoxic T-lymphocyte antigen 4 (CTLA-4), glucocorticoid-induced TNF receptor family-regulated gene (GITR), lymphocyte-activation gene 3 (LAG3), IL-21, programmed cell death 1 (PD-1) and c-masculoaponeurotic fibrosarcoma (c-Maf) expression. The expressions of molecules were given as the relative values to the calibrator samples. To standardize the amount of total RNA, we quantified β-actin mRNA from each sample as a control of internal RNA and corrected all values with this.

Induction of $CD4^+CD25^-CD127^-FOXP3^-$ T cells from PBMC

To clarify the molecular mechanisms of Treg induction, we cultured 1×10^6 naive $CD4^+CD25^-$T cells with 1×10^5 autologous monocyte-derived dendritic cells (DCs) and mitomycin C (Sigma-Aldrich, St. Louis, MO)-treated 1×10^5 HCC cell lines, Huh7 or HepG2 (AmericanType Culture Collection, Manassas, VA) on 24-well flat-bottom plates for 5 days. Monocyte-derived DCs were generated from $CD14^+$ cells as reported previously.[18] On days 2 and 4 of the coculture, recombinant human IL-2 (10 IU/ml), IL-10 (20 IU/ml) and IL-15 (20 IU/ml; BD Pharmingen) were added to the cells. On day 6, they were stimulated with phorbol 12-myristate 13 acetate (PMA; 1 ng/ml) and ionomycin (1 μmol/l) in the presence of anti-CD3 mAb (1 μg/ml) and breferdin A (1 μg/ml) (BD Pharmingen). In some experiments, we separated relevant cells by transwell inserts (pore size 0.4 μm) or added 10 μg/ml neutralizing Abs against TGF-β (R&D), HLA-DR (BD), PD-1 (R&D), programmed cell death 1 ligand 1 (PD-L1; e-Bioscience) or immunoglobulin-like transcript 4 (IL-T4) (e-Bioscience) during the culture. Subsequently, the cells were stained with Abs for CD4, CD25, CD127, FOXP3 and IL-10 and then were subjected to FACS analysis.

Knockdown of PD-L1 and HLA-G genes in HCC cell lines by siRNA

To confirm the molecules involving Treg induction, we knocked down PD-L1 and HLA-G genes in Huh7 cells by means of RNA interference. We used the small interfering RNA (siRNA) cocktail targeting human CD274 (PD-L1) or human leukocyte antigen G (HLA-G), provided by COSMO BIO (Tokyo, Japan). Transfection of siRNA to Huh7 or HepG2 cells was performed using lipofectamine RNAiMAX (Invitrogen) according to the manufacturer's instructions. To assess the efficiency of transfection, we compared the mRNA expression of target genes before and after the procedure by real time RT-PCR.

Statistical analyses

The Jonckheere-Terpstra test was used for the analysis of dose-dependent tendency. The Mann-Whitney nonparametric *U* test was used to compare differences in unpaired samples and Kruskal–Wallis nonparametric tests were used to compare differences among multiple groups, respectively. Friedman test with Bonferroni multiple comparison tests was used to compare differences in paired samples. All tests were two-tailed, and a $p < 0.05$ was considered statistically significant.

Results

$CD4^+$ T cells with distinct patterns of CD127 and FOXP3 expression were identified

According to the expression of CD25 and CD127 in $CD4^+$ T cells, we separated them into four groups: $CD25^{high+}CD127^-$, $CD25^-CD127^-$, $CD25^{high-}CD127^+$ and $CD25^-CD127^+$ cells, respectively (Fig. 1*a*). Most of the $CD4^+CD25^{high+}CD127^-$

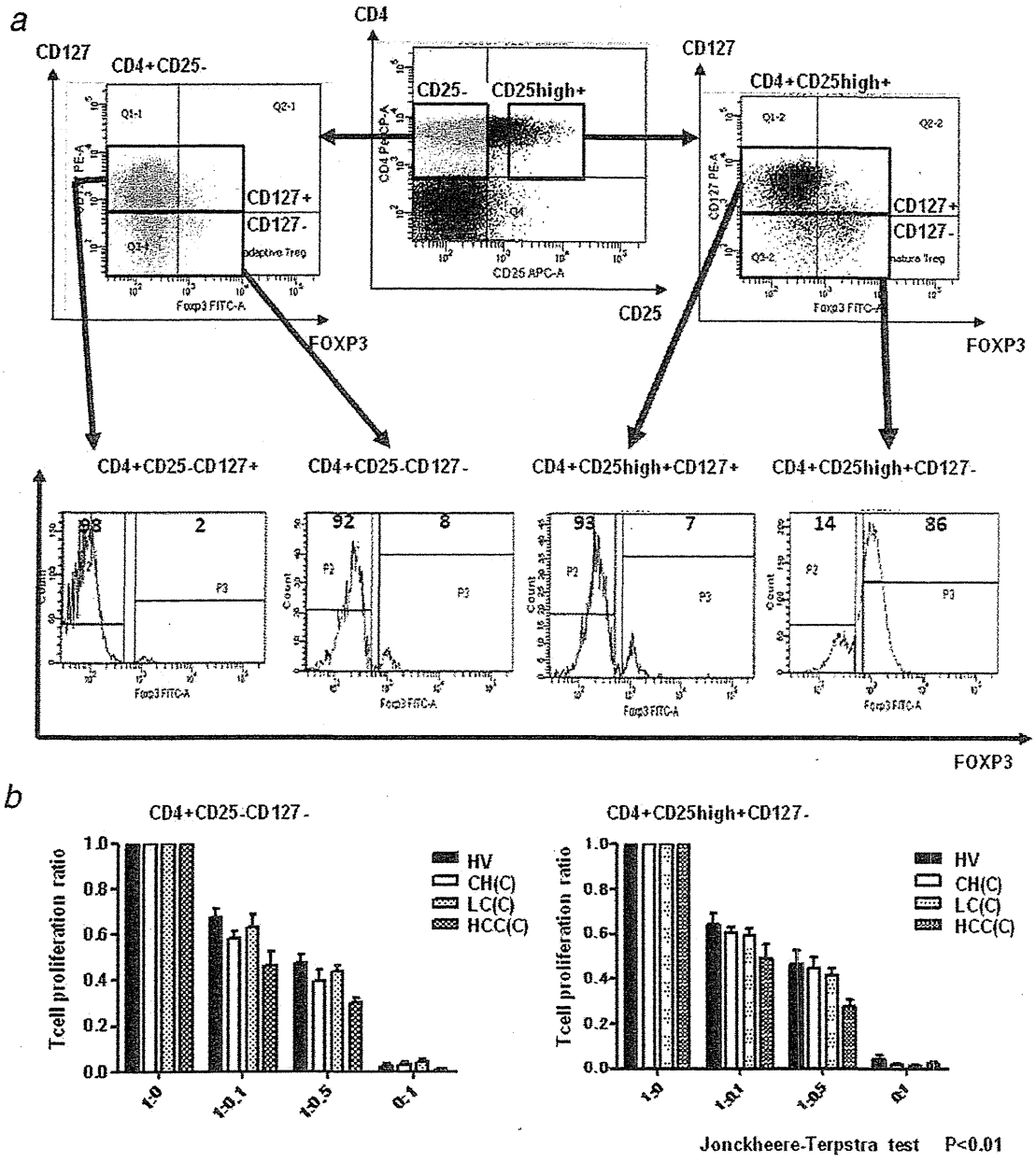

Figure 1. $CD4^+CD25^-CD127^-$ and $CD4^+CD25^{high+}CD127^-$ T cells are Tregs. (*a*) $CD4^+$ T cells are separated into four subpopulations: $CD4^+CD25^{high+}CD127^+$, $CD4^+CD25^{high+}CD127^-$, $CD4^+CD25^-CD127^+$ and $CD4^+CD25^-CD127^-$ cells, respectively. These cells were examined for FOXP3 expression. The numbers in the histograms depict the percentages of gated cells. Representative plots from three patients and donors are shown. (*b*) Sorted $CD4^+CD25^-CD127^-$ T cells and $CD4^+CD25^{high+}CD127^-$ T cells obtained from patients and healthy donors were added at various ratios to allogenic $CD4^+$ T cells stimulated with anti-CD3 and anti-CD28 Abs. After 5 days of culture, $CD4^+$ T cell proliferation was evaluated by incorporation of ^{3}H-thymidine. The bars indicate the ratio of counts per minutes (cpm) in various responders to regulatory cells ratio to those at 1:0. The results are shown as mean + SEM of ten patients or donors in each group. The dose dependency was analyzed by Jonckheere Terpstra test and comparison among the disease statuses was analyzed by Wilcoxon rank sum test with Bonferroni multiple comparison test. HV, healthy volunteers; CH(C), LC(C), HCC (C), HCV-infected chronic hepatitis, liver cirrhosis or hepatocellular carcinoma, respectively.

cells express FOXP3 (>80%). In contrast, the populations of $CD4^+CD25^-CD127^-$, $CD4^+CD25^{high+}CD127^+$ and $CD4^+CD25^-CD127^+$ lack FOXP3 expression (<10%). These results show that, except for $CD4^+CD25^{high+}CD127^-$ cells, the remaining $CD127^-$ cells lack FOXP3 and CD25 expression ($CD4^+CD25^-CD127^-FOXP3^-$).

$CD4^+CD25^{high+}CD127^-$ cells and $CD4^+CD25^-CD127^-$ T cells are suppressors against allogeneic T cells with distinct mechanisms

To examine which cell populations exert a suppressive capacity, we added each phenotype of cells separated from the subjects to allogeneic $CD4^+$ T cells. The sorted $CD4^+CD127^+$ T cells had no regulatory activities regardless of CD25 expression (data not shown). In contrast, $CD127^-$ cells, either $CD25^-$ or $CD25^{high+}$, significantly inhibited allogenic $CD4^+$ T cell proliferation in a dose-dependent manner, at comparable levels (Fig. 1*b*). Of note is that their suppressive capacity did not differ at the single cell level between patients and donors, regardless of the stage of liver disease (Fig. 1*b*). In addition, $CD127^-$ cells are anergic irrespective of CD25 expression (Fig. 1*b*). The suppressive ability of $CD4^+CD25^{high+}CD127^-$ cells was significantly abrogated by transwells and anti-TGF-β Ab, suggesting that they work in cell–cell contact-dependent and TGF-β-dependent manners (Supporting Information Fig. 1). By contrast, suppression by $CD4^+CD25^-CD127^-$ cells was alleviated by anti-IL-10 Ab but not by transwells, showing that they are contact-independent but IL-10-dependent (Supporting Information Fig. 1). These results show that $CD4^+CD25^-CD127^-$ cells possess a suppressive capacity with distinct machinery from $CD4^+CD25^{high+}CD127^-$ cells. In the setting of tetanus toxoid-reactive $CD4^+$ T cell response, each type of cells tended to be comparably suppressive (Supporting Information Fig. 2).

$CD4^+CD25^{high+}CD127^-$ and $CD4^+CD25^-CD127^-$ T cells display distinct gene profiles

$CD4^+CD25^{high+}CD127^-$ and $CD4^+CD25^-CD127^-$ T cells were sorted by FACS Aria and were subjected to real-time RT-PCR analyses. The expressions of FOXP3, CTLA-4 and GITR in $CD4^+CD25^{high+}CD127^-$ cells were higher than those in $CD4^+CD25^-CD127^-$ T cells, while those of LAG-3, IL-21, PD-1 and c-Maf in $CD4^+CD25^-CD127^-$ T cells were higher than those in $CD4^+CD25^{high+}CD127^-$ cells, respectively (Fig. 2). Thus, these two types of regulatory cells have distinct molecular profiles. As we described in the previous sections, $CD4^+CD25^-CD127^-$ cells with regulatory capacity lack FOXP3 expression (Figs. 1 and 2). Thus, we tentatively defined such cells as $CD25^-FOXP3^-$ Tregs in the following parts.

$CD25^-FOXP3^-$ Tregs are increased in HCC patients and their increments are associated with cancer progression

We compared the frequency of Treg subsets among healthy donors and HCV-infected patients. In HCC patients, $CD25^-FOXP3^-$ Tregs or $CD4^+$ $CD127^-$ $CD25^{high+}$ $FOXP3^+$ cells ($CD25^{high+}FOXP3^+$ Tregs) frequency in the periphery was significantly higher than those in other groups (Fig. 3*a*). The frequency of each type of Tregs is not correlated with HCV quantity (Supporting Information Fig. 3). These results show that the increase in $CD25^-FOXP3^-$ or $CD25^{high+}FOXP3^+$ Tregs is correlated with the development of liver cancer, but not with HCVRNA titers. Such increment of peripheral Tregs is also observed in HBV-HCC or NBNC-HCC patients (Fig. 3*a*).

Next, we compared the frequency of Tregs between PBMC and liver-infiltrating lymphocytes in HCC patients. Both $CD25^-FOXP3^-$ and $CD25^{high+}FOXP3^+$ Tregs are detected in liver-infiltrating lymphocytes, and $CD25^-FOXP3^-$ Tregs are higher in tumor-infiltrating lymphocytes than those in nontumor-infiltrating and circulating lymphocytes (Fig. 3*b*). These results demonstrate that $CD25^-FOXP3^-$ Tregs increase both in the liver and in the periphery in parallel with the development of cancer.

We serially examined the frequency of $CD25^-FOXP3^-$ Tregs and $CD25^{high+}FOXP3^+$ Tregs before and after RFA therapy. The $CD25^-FOXP3^-$ Tregs frequency dramatically decreased after successful HCC ablation and further subsided in patients without intrahepatic recurrence (Fig. 4*a*). In clear contrast, in patients with subsequent HCC recurrence, $CD25^-FOXP3^-$ Tregs increased before apparent radiological identification of HCC (Fig. 4*a*). Such dynamic frequency changes in parallel with HCC recurrence were not apparent in $CD25^{high+}FOXP3^+$ Tregs (Fig. 4*b*). Therefore, $CD25^-FOXP3^-$ Treg frequency is more closely correlated than $CD25^{high+}FOXP3^+$ Tregs with the presence or absence of HCC.

PD-L1, IL-T4 and HLA-G are involved in the induction of $CD4^+CD25^-CD127^-FOXP3^-$ IL-10^+ T cells

After the culture of naive $CD4^+$ T cells, DC and Huh7 or HepG2, we found that $CD4^+CD25^-CD127^-FOXP3^-$ cells produce IL-10 (Fig. 5*a*), whereas $CD4^+CD25^+CD127^-FOXP3^+$ cells do not (Supporting Information Fig. 4). Since $CD4^+CD25^-CD127^-$ cells use IL-10 as one of suppressor mechanisms (Supporting Information Fig. 1), such IL-10^+ $CD4^+CD25^-CD127^-FOXP3^-$ T cells are functionally competent $CD25^-FOXP3^-$ Tregs (Fig. 5*a*). In culture, the frequency of IL10^+ $CD25^-FOXP3^-$ T cells decrease in the presence of anti-TGF-β, anti-PD-1, anti-PD-L1 or anti-ILT4 Abs, with the difference being the most significant with anti-PD-L1 or anti-ILT4 Abs (Fig. 5*b*). Next, in the absence of DC or the separation of T cells from HCC cell lines significantly reduced IL10^+ $CD25^-FOXP3^-$ T cell induction, whereas separation of T cells from DC did not change it (Fig. 5*c*). These results indicate that the contact between T cells and HCC cell lines is indispensable for IL-10^+ $CD25^-FOXP3^-$ T cell induction, but the contacts between T cells and DC or between DC and HCC cell lines are not, respectively. Similarly, the addition of anti-PDL1 or anti-IL-T4 Abs to this culture resulted in suppression of IL-10^+ $CD25^-FOXP3^-$ T cell induction, regardless of the presence of transwells (Fig. 5*c*).

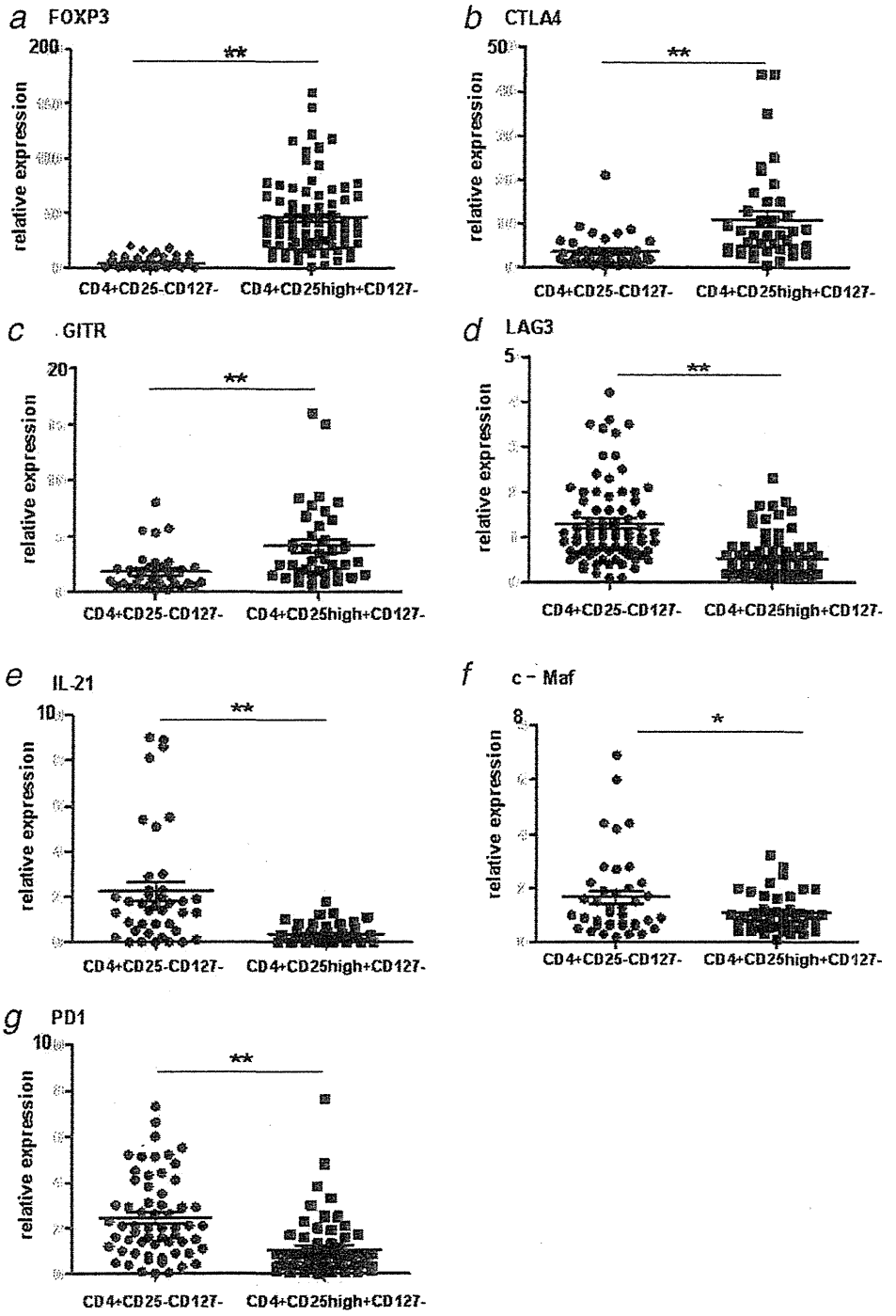

Figure 2. $CD4^+CD25^-CD127^-$ T cells and $CD4^+CD25^{high+}CD127^-$ T cells display distinct gene profiles. Sorted $CD4^+CD25^-CD127^-$ cells and $CD4^+CD25^{high+}CD127^-$ cells from PBMC of HCC patients were subjected to real-time RT-PCR for the analyses of FOXP3 (*a*), CTLA4 (*b*), GITR (*c*), LAG3 (*d*), IL-21 (*e*), c-Maf (*f*) and PD1 (*g*). The results are shown in relative expression of relevant genes to those of β-actin. *: $p < 0.05$; **: $p < 0.01$ by Mann-Whitney *U* test with Welch's correction.